The CLASS blazar survey - II. Optical properties

Caccianiga, A.; Marcha, M. J.; Anton, S.; Mack, K. H.; Neeser, M. J.

Published in:
Monthly Notices of the Royal Astronomical Society

DOI:
10.1046/j.1365-8711.2002.05062.x

Mon. Not. R. Astron. Soc. **329,** 877–889 (2002)

The CLASS blazar survey – II. Optical properties

A. Caccianiga,[1★] M. J. Marchã,[1] S. Antón,[1] K.-H. Mack[2,3,4] and M. J. Neeser[5,6]

[1]*CAAUL, Observatório Astronómico de Lisboa, Tapada da Ajuda, 1349-018 Lisboa, Portugal*
[2]*ASTRON/NFRA, Postbus 2, NL-7990 AA Dwingeloo, the Netherlands*
[3]*Istituto di Radioastronomia del CNR, Via P. Gobetti 101, I-40129 Bologna, Italy*
[4]*Radioastronomisches Institut der Universität Bonn, Auf dem Hügel 71, D-53121 Bonn, Germany*
[5]*Kapteyn Astronomical Institute Postbus 800, NL-9700 AV Groningen, the Netherlands*
[6]*Universitäts-Sternwarte München, Scheinerstrasse 1, D-81679 München, Germany*

Accepted 2001 October 8. Received 2001 August 24; in original form 2001 April 19

ABSTRACT

This paper presents the optical properties of the objects selected in the CLASS blazar survey. Because an optical spectrum is now available for 70 per cent of the 325 sources present in the sample, a spectral classification, based on the appearance of the emission/absorption lines, is possible. A wide variety of optical spectral types is found. Besides 'classical' BL Lacs (42), BL Lac candidates (5) and high-power ($P_{5\,\mathrm{GHz}} > 10^{26}\,\mathrm{W\,Hz^{-1}}$) flat spectrum radio quasars (67), a significant number of 'passive' elliptical galaxies (41) is also found. Moreover, 33 broad emission line objects with a low radio power ($P_{5\,\mathrm{GHz}} < 10^{26}\,\mathrm{W\,Hz^{-1}}$) are discovered, suggesting that at least a fraction (~24–30 per cent) of low-power blazars have a broad line region. Finally, 34 objects showing only narrow emission lines, either as a result of some starburst activity in the host galaxy or as a result of the presence of an active galactic nucleus, appear in the sample.

Key words: surveys – galaxies: active – BL Lacertae objects: general – quasars: general.

1 INTRODUCTION

The Cosmic Lens All Sky Survey (CLASS; Myers et al., in preparation) is a deep ($S_{5\,\mathrm{GHz}} > 30\,\mathrm{mJy}$) survey of flat spectrum radio sources created with the primary aim of selecting new gravitational lens systems in the radio band. Nevertheless, the CLASS survey can also be used to study the statistical properties of flat spectrum active galactic nuclei (AGNs), usually called *blazars*, including BL Lac objects and flat spectrum radio quasars (FSRQ). In the first paper (Marchã et al. 2001, hereafter Paper I) of this series, a well defined sample of 325 optically bright ($R \leqslant 17.5$) CLASS sources has been presented. As discussed in Paper I, this sample is selected in order to study the low-luminosity tail of the blazar class. Thanks to its low flux limit, a factor ~30 below the 1-Jy sample of radio sources (Kühr et al. 1981) and a factor ~6 below the 200-mJy sample (Marchã et al. 1996), the CLASS sample of blazars offers a unique opportunity of exploring the properties of blazars with a radio power as low as $\sim 10^{23}\,\mathrm{W\,Hz^{-1}}$. At these levels of power it is not clear whether the range of properties observed in more powerful objects are still the same. For instance, the results of the analysis of the 200-mJy sample of blazars has revealed a surprising variety of optical properties unexpected on the basis of the 'standard' unification schemes. In particular, a high fraction (~20 per cent) of objects with broad emission lines have been found in a range of power ($P_{5\,\mathrm{GHz}} < 10^{26}\,\mathrm{W\,Hz^{-1}}$) usually covered by featureless blazars (i.e. BL Lac objects). However, given the relatively small number of objects contained in the 200-mJy sample, the high percentage of objects with broad emission lines found in the sample could be a statistical fluctuation. The aim of the CLASS blazar survey is to put the investigation of the properties of low-luminosity blazars on a firmer statistical basis. This paper presents the optical properties of the 237 objects, out of 325 sources in the optically bright CLASS sample, for which an optical spectrum or a classification from the literature has been collected. In Section 2 the defining criteria used to select the CLASS sample are summarized, while in Section 3 and 4 the optical observations and the classification criteria are presented and discussed. In Section 5 the radio and optical luminosities for the different classes of objects are analysed. The conclusions are summarized in Section 6.

Throughout this paper $H_0 = 50\,\mathrm{km\,s^{-1}\,Mpc^{-1}}$ and $q_0 = 0$ are used.

2 THE CLASS SAMPLE OF BLAZARS

In Paper I the CLASS sample of optically bright sources has been presented and discussed. In summary, 325 flat spectrum radio sources were selected with the following criteria;

(i) $35° \leqslant \delta \leqslant 75°$,
(ii) $|b^{II}| \geqslant 20°$,

★E-mail: caccia@oal.ul.pt

Table 1. Summary of the observations.

Telescope/Instrument	Grism name (gr mm^{-1})	Dispersion (Å pixel^{-1})	Observing Period	note[a]	code[b]
INT+IDS+TEK3	R300V (300)	3.3	1997 Jul 5–12		INT7/97
INT+IDS+TEK3	R300V (300)	3.3	1998 Feb 15–21		INT2/98
INT+IDS+TEK5	R300V (300)	3.3	1999 Feb 25–27	CCI	INT2/99
INT+IDS+TEK5	R300V (300)	3.3	1999 May 7–11	CCI	INT5/99
Calar Alto 2.2 m+CAFOS	B200/R200 (200)	4.5	1999 Jun 29–Jul 6		CA7/99
NOT+ALFOSC	G4 (300)	3.3	1999 Aug 20–25	CCI	NOT8/99
INT+IDS+TEK5	R300V (300)	3.3	1999 Oct 20	CCI	INT10/99
INT+IDS+EEV10	R300V (300)	3.7	2000 Feb 17	CCI	INT2/00

[a]CCI = the observing run belongs to the International Collaborative Programme.
[b]This code is used in column 8 of Table 2.

(iii) $S_5 \geqslant 30$ mJy,
(iv) flat spectrum, i.e. $\alpha_{1.4}^{4.8} \leqslant 0.5 (S_\nu \propto \nu^{-\alpha})$, and
(v) red magnitude $\leqslant 17\overset{\mathrm{m}}{.}5$.

The catalogues used for the selection process are the GB6 catalogue (Gregory et al. 1996) at 4.8 GHz and the NRAO VLA Sky Survey (NVSS) catalogue (Condon et al. 1998) at 1.4 GHz. The APM red magnitudes have been corrected in order to minimize the systematic errors on the magnitudes of extended sources (see Paper I). Moreover, an accurate analysis of the combined positional uncertainties of the NVSS and APM catalogues has been performed in order to set the correct correlation tolerance used to define the optical counterpart. We estimate a completeness level of ~95 per cent.

3 OBSERVATIONS

Several observing runs were carried out in the past years with the aim of collecting a spectroscopic classification and redshift for the CLASS objects. In particular, the CLASS project has obtained observing time at the telescopes in La Palma and Tenerife (Canary Islands, Spain) in the context of the International Collaborative Programme, which allocates 5 per cent of the total observing time of the telescopes to one or more international programme each year. As far as the sample presented here is concerned, the Isaac Newton Telescope (INT) and the Nordic Optical Telescope (NOT) were used. Other observations have been carried out at the 2.2-m telescope in Calar Alto (Spain).

In all cases a long-slit and low-dispersion grism (3–5 Å pixel^{-1}) were used in order to maximize the wavelength coverage. Each spectrum was reduced to its final flat-fielded, wavelength and flux-calibrated form using standard methods within the IRAF software package. A summary of the observations is given in Table 1.

A total of 99 sources from the sample presented here were observed and classified. Except for a few featureless spectra (BL Lac objects), a redshift was secured for all these sources. A further 138 identifications have been found from the literature making use of the NED facility.[1] Among these 138 objects, 10 are generically classified as ‘galaxies’ without a published optical spectrum available. For these objects a spectroscopical follow-up will be necessary in order to have a more accurate classification.

In total, 227 sources out of 325 (70 per cent) have a classification, plus 10 for which a redshift is available but not an optical classification.

[1] NED is operated by the Jet Propulsion Laboratory, Caltech, under contract to NASA

4 SOURCE CLASSIFICATION

On the basis of the optical spectrum the sources have been divided in three main groups:

(i) *Type 0* objects, whose optical spectrum does not show any strong emission lines, i.e. if present, an emission line must have an equivalent width (EW) less than 5 Å. This class of objects includes both the featureless BL Lac objects and some apparently ‘normal’ elliptical galaxies whose spectra show only absorption features.
(ii) *Type 1*, which includes sources with broad emission lines (full width at half maximum, FWHM, $\geqslant 1000\,\mathrm{km\,s^{-1}}$) in the optical spectrum, i.e. typical radio-loud quasi-stellar objects (RL QSOs), broad line radio galaxies (BLRGs) and Seyfert 1 galaxies (Sy1).
(iii) *Type 2*, which contains the objects with only narrow emission lines (*FWHM* $< 1000\,\mathrm{km\,s^{-1}}$) in the optical spectrum. This group is the most heterogeneous one and includes Seyfert 2 galaxies (Sy2s), narrow-line radio galaxies (NLRGs), H II-region galaxies and starburst galaxies.

The three classes are discussed in the next sections.

4.1 Type 0

Type 0 objects are further classified as BL Lacs, BL Lac candidates and ‘passive elliptical galaxies’ (PEGs) on the basis of the value of the Calcium break at 4000 Å(Δ), which is defined as in Dressler & Shectman (1987), i.e.

$$\Delta = \frac{S^+ - S^-}{S^+}, \tag{1}$$

where S^+ and S^- represent the mean value of the flux density (expressed per unit frequency) in the region 4050–4250 and 3750–3950 Å (in the rest-frame of the source) respectively.

All the type 0 objects with Δ below 25 per cent were classified as BL Lac objects, according to the ‘classical’ definition proposed by Stocke et al. (1991). Nevertheless, it has been recently shown by different authors (Marchã et al. 1996; Laurent-Muehleisen et al. 1998; Caccianiga et al. 1999) that this limit can miss a significant fraction of weak BL Lacs. A higher limit on Δ (40 per cent) has been suggested and used by many authors to classify an object as BL Lac (or BL Lac candidate). According to this, all the type 0 objects in the CLASS blazar survey with a value of Δ between 25 and 40 per cent are classified as ‘BL Lac candidates’. Finally, the type 0 objects with a value of Δ larger than 40 per cent were classified as PEGs. This (arbitrary) distinction based on the value of Δ has been applied to the objects in the CLASS blazar survey for consistency with the classification usually found in the literature.

It is worth noting that, given the limited wavelength coverage, there can be an ambiguity in the classification of an object as type 0. In particular, a type 1 object with a broad Hα can be misclassified as type 0 (PEG) if the region around 6563 Å (in the rest frame of the source) is not covered. However, only nine objects classified as PEGs have a wavelength coverage that does not include the region where Hα is expected to be found. Hence, although the classification as type 0 can change if Hα in emission is found in these objects with the proper spectral coverage, the results discussed in this paper will not be significantly affected.

4.2 Type 1

This class contains both strong emission line objects ($EW > 80$ Å) and sources with much weaker emission lines ($EW \leqslant 80$ Å). For the latter, the assessment of the actual linewidth is more problematic. In fact, in most of these objects the only group of lines detected in the optical spectrum is the Hα + [N II] group. Because the two [N II] lines are often blended with the Hα line, the measurement of the actual width of the Hα line is not simple. Recently, a systematic follow up of the 6563-Å region for many nearby galaxies by Ho et al. (1997) has revealed that, after a proper de-blending of the Hα + [N II] group of lines, a broad component in the Hα line is often found.

In the CLASS bright sample, 21 objects have $z < 0.21$ and a Hα + [N II] line blend with $EW \leqslant 80$ Å. For these objects the classification as type 1 is more difficult, although in six cases the presence of a broad Hα line is claimed in the literature. In principle, the detection of a broad Hα component in the Hα + [N II] line blend would require a proper treatment that is not allowed by the quality of the data presented here. As described by Ho et al. (1997), in order to extract a weak broad Hα component with $FWHM \sim 1000–3000\,\mathrm{km\,s^{-1}}$ and comprising $\geqslant$20 per cent of the flux of the Hα + [N II] blend, a good signal-noise-ratio (S/N) and spectral resolution are needed besides an accurate starlight subtraction.

However, the procedure described in Ho et al. (1997) was designed to reveal weak, broad Hα components in nearby galaxies that show no clear evidence of nuclear activity and for which the Hα + [N II] groups appear rather narrow at a visual inspection. Instead, in the case of the 'possible' type 1 objects selected in the CLASS blazar survey, a qualitative inspection of the Hα profile is more indicative for the presence of a broad component. For these sources, a more crude fitting procedure than that proposed by Ho et al. (1997) can be successful in revealing any broad components.

Thus, the Hα region has been further analysed for five out of 20 objects for which we have obtained a spectrum. A fitting procedure with two different models was applied: The first model includes just three narrow lines ([N II]λ6548, Hα, [N II]λ6583) while in the second model an additional broad Hα line is added. All the profiles are assumed to be Gaussian and no attempts of subtracting the starlight have been made.

The two models were applied to the five spectra, keeping the positions of the three lines fixed and their width and relative intensity free to vary. The width of the three narrow components is constrained to be less than $1000\,\mathrm{km\,s^{-1}}$. The results of the application of the second model to the data are shown in Fig. 1.

In four cases (GBJ022525+37029, GB6J061641+663024, GB6J165547+444735 and GB6J191212+660826), the first model is not able to fit the tails of the group of lines: for these objects the second model, containing an additional broad Hα line, which takes into account the external wings, is able to give a

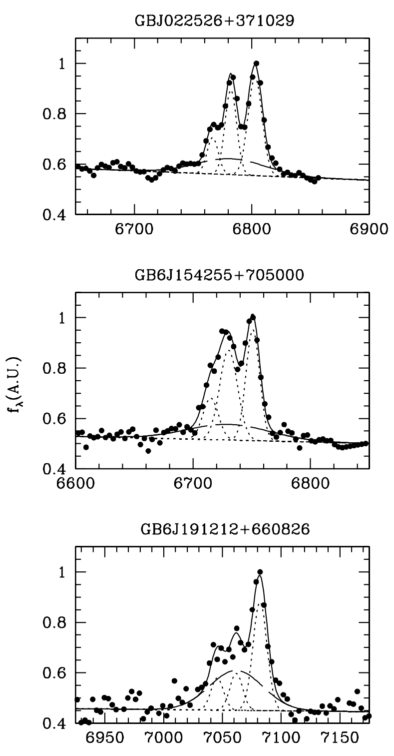

Figure 1. Results of the fitting procedure described in the text, as applied to the Hα region of the five observed type 1 candidates. The Hα + [N II] lines (points) are fitted with three narrow components (short dashes) plus a broad Hα component (long dashes). Fluxes are per unit of wavelength and given in arbitrary units.

Table 2. Identified CLASS sources. The Notes can be found in the Appendix.

Name	Other name	Type	Class	z	Log $P_{1.4}$ (W Hz^{-1})	M_R	Observation	Notes
GB6J002538+400830		0?	PEG?	0.100	24.20	−23.76	INT10/99	1
GB6J011216+381910	RGBJ0112+383	1	AGN	0.333	25.46	−24.56		2
GB6J011920+385253		0?	PEG?	0.103	24.67	−23.79	INT10/99	3
GB6J012626+395406		0?	PEG?	0.113	25.01	−22.96	INT10/99	4
GB6J013631+390623	RGBJ0136+391	0	BL	–	–	–	INT10/99	5
GB6J014156+392325	RGBJ0141+393	1	AGN	0.080	24.52	−24.07		6
GB6J015451+362746		0?	PEG?	0.118	25.16	−24.09	INT10/99	7
GB6J021625+400101		0	PEG	0.050	23.66	−23.05	INT10/99	8
GB6J022526+371029	CGCG523−037	1	AGN	0.033	23.98	−22.53	INT10/99	9
GB6J055253+724045	CJ20546+726	1	AGN	1.555	27.91	−28.73		10
GB6J061641+663024		1	AGN	0.014	23.38	−21.17	INT10/99	11
GB6J064204+675834	JVASJ0642+6758	1	AGN	3.180	27.67	−31.44		12
GB6J065010+605001	NGC2273	2	AGN	0.006	22.03	−20.49		13
GB6J065422+504223		–	star	–	–	–	INT10/99	14
GB6J065648+560258		2	G	0.056	23.88	−21.70	INT2/00	15
GB6J065817+501641		0	PEG	0.091	24.23	−22.78	INT2/00	16
GB6J070105+693634		1	AGN	1.971	28.20	−29.49		17
GB6J071044+422053	JVAS J0710+4220	1	AGN	1.163	27.44	−27.74		18
GB6J071045+473203		1	AGN	1.292	27.95	−30.43		19
GB6J071433+740811	JVAS J0714+7408	1	AGN	0.371	25.78	−24.81		20
GB6J071510+452554		0	PEG	0.052	23.95	−23.02	INT2/00	21
GB6J072151+712036	JVAS J0721+7120	0	BL	–	–	–		22
GB6J072849+570124	JVAS J0728+5701	1	AGN	0.426	26.62	−25.79		23
GB6J073502+475011	JVAS J0735+478	1	AGN	0.782	27.02	−26.62		24
GB6J073654+653603	NGC2403	2	G	0.0043	19.66	−18.13		25
GB6J073728+594106	UGC3927	1?	AGN	0.041	24.61	−23.31		26
GB6J074904+451027	RGBJ0749+451	1	AGN	0.190	25.42	−23.34		27
GB6J080053+392433		0	PEG	0.064	23.99	−24.68	INT2/00	28
GB6J080132+473624		1	AGN	0.158	24.94	−23.41		29
GB6J080624+593059	RGBJ0806+595	0	BL	–	–	–		30
GB6J080839+495033	OJ+508	1	AGN	1.430	28.03	−28.34		31
GB6J080949+521856	RGBJ0809+523	0	BL	0.138	25.18	−24.04		32
GB6J081622+573858	RGBJ0816+576	0	BL	–	–	–		33
GB6J082437+405712		1	AGN	0.613	26.53	−26.05		34
GB6J083411+580318		2?	G	0.093	24.33	−23.11		35
GB6J083455+553430	RGBJ0834+555	2	AGN?	0.242	27.35	−23.88		36
GB6J084124+705345	HB0836+710	1	AGN	2.172	29.22	−29.86		37
GB6J084215+452547	HB0838+456	1	AGN	1.406	26.98	−28.56		38
GB6J084356+510522		0	PEG	0.126	25.16	−23.36	INT2/99	39
GB6J085008+593054	HS0846+5942	1	AGN	1.710	26.27	−29.86		40
GB6J085317+682824	CGCG332 − 026	0	PEG	0.039	24.28	−24.82		41
GB6J090615+463633	JVAS 0902+468	2	G	0.085	24.97	−21.97		42
GB6J090650+412426	CGCG209 − 027	?	G	0.028	23.24	−21.60		43
GB6J090757+493558	RGB J0907+495	?	G	0.035	23.37	−21.66		44
GB6J092230+710926	87GB091749.7+712216	1	AGN	2.432	27.48	−30.27		45
GB6J092914+501323	CJ2 0925+504	0	BL	–	–	–		46
GB6J093254+673654	NGC2892	?	G	0.023	23.73	−23.54		47
GB6J094319+361447	NGC2965	2?	G	0.022	23.21	−22.73	INT2/98	48
GB6J095227+504837	SBS 0949+510	1	AGN	1.546	27.00	−28.64		49
GB6J095531+690357	NGC3031,M81	2	AGN	0.0001	18.58	−16.00		50
GB6J095552+694047	M82	2	G	0.0007	22.11	−19.05		51
GB6J095736+552258	HB 0954+556	1	AGN	0.909	28.18	−27.29		52
GB6J095847+653405	HB 0954+658	0	BL	0.368	26.59	−25.51		53
GB6J100055+533158	SBS 0957+537	1	AGN	1.348	27.13	−28.27		54
GB6J100308+681313	87GB 095911.5+682744	1	AGN	0.773	26.50	−27.79	INT2/98	55
GB6J101028+413230		1	AGN	0.612	26.84	−26.52		56
GB6J101244+423009	RGBJ1012+424	0	BL	–	–	–		57
GB6J101504+492606	RGBJ1015+494	0	BL	0.200	25.83	−23.93		58
GB6J101859+591126		0?	BL?	–	–	–		59
GB6J102310+394759		1	AGN	1.254	28.05	−28.12		60
GB6J102521+372641	CGCG183 − 022	0	PEG?	0.044	23.74	−22.70		61
GB6J103053+411300		0	PEG	0.092	24.27	−24.39	INT2/00	62
GB6J103118+505350	87GB 102814.4+510859	0	BL	0.361	25.35	−25.28	INT2/98	63
GB6J103123+744158	JVAS 1027+749	1	AGN	0.123	25.15	−22.47		64
GB6J103550+375646		1	AGN	1.508	26.94	−28.56		65
GB6J103742+571158	87GB 103431.3+572750	0	BL	–	–	–	INT2/98	66
GB6J104630+544953		2	G	0.249	25.34	−24.27	INT5/99	67
GB6J105344+493006	MS1050.7+4946	0	C−BL	0.140	24.74	−24.05		68
GB6J105430+385500		0	BL	1.363	26.80	−28.44		69
GB6J105730+405631	NGC3468	?	G	0.008	22.12	−21.76		70

Table 2 – *continued*

Name	Other name	Type	Class	z	Log $P_{1.4}$ (W Hz^{-1})	M_R	Observation	Notes
GB6J105837+562817	RGBJ1058+564	0	BL	0.144	25.31	−23.72		71
GB6J110147+722536	HB1058+726	1	AGN	1.460	28.26	−28.48		72
GB6J110242+594132	87GB 105939.4+595738	1	AGN	1.830	27.94	−29.24		73
GB6J110428+381228	MRK421	0	BL	0.030	24.50	−23.01		74
GB6J111206+352707	NGC3569	0	PEG	0.025	23.24	−22.91	INT2/99	75
GB6J111914+600459	JVAS J1119+6004	1	AGN	2.638	28.27	−30.51		76
GB6J112047+421206	RGBJ1120+422	0	BL	0.124?	24.19	−22.21		77
GB6J112413+513350		0?	C-BL	0.234	25.14	−23.97	INT5/99	78
GB6J112832+583322	NGC3690,MRK171	2	G	0.010	23.50	−22.19		79
GB6J113626+700931	MRK180	0	BL	0.046	24.49	−23.34		80
GB6J113629+673707	RGBJ1136+676	0	C-BL	0.135	24.56	−23.03		81
GB6J114047+462207		1?	AGN?	0.115	24.77	−23.29		82
GB6J114115+595309	NGC3809	?	G	0.011	22.83	−19.96		83
GB6J114300+730413		0?	PEG?	0.123	24.52	−22.57	INT5/99	84
GB6J114722+350109	JVAS J1147+3501	1?	AGN	0.063	25.04	−21.95		85
GB6J114850+592459	NGC3894	1?	AGN	0.011	23.38	−19.91		86
GB6J114856+525432	CJ2 1146+531	1	AGN	1.632	26.74	−29.51		87
GB6J115037+653916		1	AGN	2.210	27.46	−30.15	INT2/98	88
GB6J115126+585913	RGBJ1151+589	0	BL	–	–	–	INT2/98	89
GB6J115757+552713	NGC3998	1	AGN	0.003	21.72	−20.12		90
GB6J120209+444452	B31159+450	0	BL	–	–	–		91
GB6J120304+603130	JVAS J1200+608	2?	AGN	0.066	24.55	−22.04		92
GB6J120334+451050	RGBJ1203+451	1	AGN	1.070	26.32	−27.51		93
GB6J120922+411938	CJ21206+415	0	BL	–	–	–		94
GB6J121008+355224	NGC4148	?	G	0.017	22.48	−19.60		95
GB6J121108+503000	SN1937A in NGC4157	–	SN	0.003	20.18	−18.78		96
GB6J121331+504446	NGC4187	?	G	0.030	23.59	−23.83		97
GB6J121541+361924	NGC4214/NGC4228	2	G	0.001	20.15	−13.50		98
GB6J121736+515502	SBS 1215+521	1	AGN	1.090	26.78	−27.98	INT2/98	99
GB6J122208+581427		2	G?	0.100	24.35	−22.10	INT5/99	100
GB6J122306+582659	NGC4335	?	G	0.015	23.14	−22.86		101
GB6J122405+500130		1	AGN	1.062	26.52	−27.55	INT5/99	102
GB6J123012+470031	CGCG244 − 025	2	AGN?	0.039	23.80	−23.86		103
GB6J123132+641421	MS 1229.2+6430	0	BL	0.170	24.89	−23.75		104
GB6J123350+502630	JVAS 1231+507	0	PEG	0.208	25.76	−23.25		105
GB6J123413+475408	JVASJ1234+4753	1	AGN	0.375	26.37	−24.92		106
GB6J123417+505441		2	AGN?	0.172	24.95	−23.31	INT5/99	107
GB6J124036+695837	JVAS 1238+702	1	AGN	1.471	27.06	−28.42		108
GB6J124307+731549	8C 1241+735	0	PEG	0.075	25.09	−24.14		109
GB6J124313+362755	RGB J1243+364	0	BL?	–	–	–		110
GB6J124732+672322	JVAS 1245+676	0	PEG	0.107	25.13	−22.51		111
GB6J124818+582029	PG 1246+586	0	BL	–	–	–	INT2/98	112
GB6J125311+530113	CJ2 1250+532	0	BL	–	–	–	INT5/99	113
GB6J125614+565220	MRK231	1	AGN	0.042	24.38	−24.25		114
GB6J130132+463357		1?	AGN?	0.206	25.16	−23.97	CA7/99	115
GB6J130836+434405	NGC5003	2?	G	0.035	23.49	−24.03	INT2/99	116
GB6J130924+430502		0	BL?	–	–	–	INT7/97	117
GB6J131215+445023	CGCG245 − 031	0	PEG	0.035	23.86	−24.39		118
GB6J131218+351522	RGBJ1312+352	1	AGN	0.184	24.86	−23.69		119
GB6J131328+363538	NGC5033	1?	AGN	0.003	21.65	−22.22		120
GB6J131655+722619		1	AGN	1.990	26.71	−29.41	INT2/98	121
GB6J131739+411538	JVAS J1317+4115	0	PEG	0.067	24.72	−24.67	CA7/99	122
GB6J131947+514759	HB 1317+520	1	AGN	1.060	27.93	−27.55		123
GB6J134139+371653		0	PEG	0.170	25.21	−23.08	CA7/99	124
GB6J134442+402811		0	PEG	0.076	24.34	−24.81	CA7/99	125
GB6J134444+555322	MRK273	2	AGN	0.038	23.95	−23.30		126
GB6J134856+395904	NGC5311	?	G	0.009	22.47	−21.55		127
GB6J134913+601114	NGC5322	2	AGN	0.006	22.15	−18.38		128
GB6J134934+534125	HB 1347+539	1	AGN	0.980	27.83	−27.31		129
GB6J135251+654124		2	AGN	0.206	25.42	−23.57	INT5/99	130
GB6J135313+350912		0	PEG?	0.139	24.58	−23.51	CA7/99	131
GB6J135327+401700	NGC5353	2	AGN?	0.008	22.02	−22.42		132
GB6J135607+413637	RGBJ1356+416	1	AGN	0.697	25.70	−26.85	INT7/97	133
GB6J140850+650550		1	AGN	1.010	26.17	−27.36	INT7/97	134
GB6J141132+742404		0	BL	–	–	–	INT5/99	135
GB6J141159+423952	RGBJ1411+426	1	AGN	0.888	26.67	−27.28	INT7/97	136
GB6J141343+433959	87GB1411+4354	1	AGN	0.089	24.22	−22.67		137
GB6J141536+483102	RGBJ1415+485	0	BL	–	–	–	INT7/97	138
GB6J141946+542328	PG 1418+546	0	BL	0.151	25.88	−24.41		139
GB6J142312+505543	JVAS 1421+511	1	AGN	0.274	26.03	−24.71		140

Table 2 – *continued*

Name	Other name	Type	Class	z	Log $P_{1.4}$ (W Hz^{-1})	M_R	Observation	Notes
GB6J142814+391222		0	PEG	0.260	25.90	−23.76	CA7/99	141
GB6J143120+395245		1	AGN	1.212	27.16	−28.61	INT7/97	142
GB6J143239+361823	NGC5675	2	AGN?	0.013	22.95	−21.01		143
GB6J143646+633645	HB 1435+638	1	AGN	2.068	28.47	−29.61		144
GB6J143920+371148		1	AGN	0.990	26.39	−27.25	INT7/97	145
GB6J144920+422103	87GB14474+4233	2	AGN	0.178	25.35	−23.10		146
GB6J150411+685605	RGBJ1504+689	1	AGN	0.318	25.72	−24.54	INT7/97	147
GB6J150522+604007		0	PEG	0.159	24.82	−24.37	INT2/99	148
GB6J150914+700436		2	G?	0.025	23.24	−21.10		149
GB6J151554+561850	NGC5907	2	G	0.002	21.06	−19.50		150
GB6J151746+652456	1ES 1517+656	0	BL	0.702	25.96	−26.34	INT7/97	151
GB6J151806+424346	VV705	2	G	0.040	23.55	−23.62		152
GB6J151807+665746		2	G	0.057	23.73	−24.81	INT2/99	153
GB6J151838+404532	RGBJ1518+407	1	AGN	0.065	23.90	−22.57		154
GB6J152911+693455		1	AGN	2.400	27.16	−30.22	INT7/97	155
GB6J153134+720634	JVAS J1531+7206	1	AGN	0.899	27.19	−26.96		156
GB6J153900+353053		1?	AGN?	0.080	24.43	−21.99		157
GB6J154255+612950	RGBJ1542+614	0	BL	–	–	–	INT7/97	158
GB6J154255+705000		1?	AGN?	0.025	23.09	−23.06	INT2/99	159
GB6J154504+525930		2	AGN	0.291	25.93	−24.02	INT5/99	160
GB6J155158+580642		1	AGN	1.324	27.05	−28.90		161
GB6J155722+544043		0	PEG	0.047	24.04	−23.65	INT2/00	162
GB6J155848+562524	JVAS 1557+565	0	PEG	0.300	25.91	−24.27		163
GB6J155901+592437	JVAS 1558+595	0?	PEG?	0.060	24.54	−24.97		164
GB6J155922+731026		0?	PEG?	0.193	24.89	−23.73	INT5/99	165
GB6J160318+694552		1	AGN	1.185	27.20	−28.15	INT5/99	166
GB6J160357+573101	HB87 1602+576	1	AGN	2.850	28.20	−30.70		167
GB6J160820+601834		1	AGN	0.180	24.94	−23.68	INT7/97	168
GB6J161447+374554		1	AGN	1.525	26.89	−29.36	INT7/97	169
GB6J161941+525617		1	AGN	2.340	27.93	−30.04	INT7/97	170
GB6J161947+523319		0	PEG	0.064	23.89	−23.25	CA7/99	171
GB6J162025+690512		1	AGN	1.490	27.06	−28.80	INT7/97	172
GB6J162303+662411	JVAS J1623+6624	1	AGN	0.201	25.36	−23.61		173
GB6J162308+390946	RGBJ1623+391	1	AGN	1.970	27.48	−30.23		174
GB6J162509+405345	NGC6146	0	PEG	0.030	23.77	−24.02	CA7/99	175
GB6J162612+512044	RGBJ1626+513	1	AGN	0.179	24.87	−23.04		176
GB6J162636+580914		1	AGN	0.748	27.25	−27.45		177
GB6J163801+552547		?	G?	0.030	23.80	−22.71		178
GB6J163813+572029		1	AGN	0.751	27.43	−26.87		179
GB6J164220+665608		1	AGN	1.895	27.62	−29.43	INT7/97	180
GB6J164258+394842	RGBJ1642+398	1	AGN	0.593	28.02	−27.20		181
GB6J164420+454644	RGBJ1644+457	0	BL	0.223	25.65	−23.80		182
GB6J164734+494954	JVAS J1647+499	1	AGN	0.048	24.25	−20.83		183
GB6J165138+400227		1	AGN	2.316	27.10	−29.99		184
GB6J165353+394541	MRK501	0	BL	0.034	24.89	−25.06		185
GB6J165547+444735		1	AGN	0.076	23.98	−23.22	CA7/99	186
GB6J165721+570556		1	AGN	1.281	27.95	−28.10		187
GB6J165728+741302		2	G?	0.159	23.85	−23.07	INT5/99	188
GB6J170123+395432		0	BL	–	–	–	INT7/97	189
GB6J170449+713840		0	BL?	–	–	–	CA7/99	190
GB6J170716+453607	JVAS J1707+4536	1	AGN	0.648	27.28	−26.11		191
GB6J171523+572434	NGC6338	0	PEG	0.027	23.30	−24.89	CA7/99	192
GB6J171613+683636	RGBJ1716+686	1	AGN	0.777	27.03	−26.68		193
GB6J171718+422711	RGBJ1717+424	2	AGN	0.183	25.29	−24.40	NOT8/99	194
GB6J171813+422759		1?	AGN?	0.180	25.21	−23.11	CA7/99	195
GB6J171914+485839	UGC10814	1	AGN	0.024	23.56	−22.07		196
GB6J171937+480404	RGBJ1719+480	1	AGN	1.084	26.43	−28.80		197
GB6J171941+354700		0?	PEG?	0.269	25.05	−23.91	CA7/99	198
GB6J172110+354217	RGBJ1721+357	1	AGN	0.263	26.40	−24.08		199
GB6J172315+654751		1	AGN	1.450	27.51	−28.89	INT7/97	200
GB6J172535+585127		0	BL	–	–	–	INT7/97	201
GB6J172722+551059		2	AGN?	0.247	25.53	−23.80	INT5/99	202
GB6J172818+501315	I Zw 187	0	BL	0.055	24.49	−21.99		203
GB6J172859+383819	RGBJ1728+386	1	AGN	1.390	27.41	−28.48		204
GB6J173047+371451		0	BL	–	–	–	CA7/99	205
GB6J173234+712359	RGBJ1732+714	0	PEG	0.060	24.45	−23.55	NOT8/99	206
GB6J173312+704632	WN B1733+7048	0	PEG	0.040	23.74	−22.41	NOT8/99	207
GB6J174113+722447		0	C-BL	0.220	25.31	−23.37	INT5/99	208
GB6J174231+594513	RGBJ1742+597	0	BL	–	–	–	CA7/99	209
GB6J174455+554220	NGC6454	1?	AGN?	0.031	24.46	−23.96		210

Table 2 – *continued*

Name	Other name	Type	Class	z	Log $P_{1.4}$ (W Hz^{-1})	M_R	Observation	Notes
GB6J174832+700550	RGBJ1748+700	0	BL	0.770	27.31	−27.10		211
GB6J174900+432151	CJ21747+433	0	BL	–	–	–		212
GB6J175131+471259	RGBJ1751+472	1	AGN	1.480	26.74	−28.79		213
GB6J175546+623652	NGC6521	1?	AGN	0.027	23.97	−25.11		214
GB6J175628+580708		2	G?	0.192	24.93	−23.61	INT5/99	215
GB6J175704+535153	RGBJ1757+538	0?	PEG?	0.119	24.57	−24.32		216
GB6J175728+552309	RGBJ1757+553	0	PEG	0.065	24.17	−23.91	INT5/99	217
GB6J175833+663801	NGC6543	–	PN	0.000	0.00			218
GB6J180132+440409	RGBJ1801+440	1	AGN	0.663	27.07	−26.39		219
GB6J180228+481932		2	AGN?	0.129	24.14	−23.08	NOT8/99	220
GB6J180557+574749		0	PEG	0.110	24.69	−22.21	NOT8/99	221
GB6J180651+694931	3C371	0	BL	0.051	25.35	−22.42		222
GB6J181156+521431		1	AGN	1.210	26.69	−28.24	INT7/97	223
GB6J181912+551103		1	AGN	1.670	27.11	−29.29	INT7/97	224
GB6J183850+480237	RGBJ1838+480	0	BL	–	–	–		225
GB6J183858+573535		0	C-BL	0.164	25.01	−23.20	INT5/99	226
GB6J184033+621257		0?	PEG?	0.050	23.86	−20.94	NOT8/99	227
GB6J184917+670548	RGBJ1849+670	1	AGN	0.657	26.93	−27.12		228
GB6J184941+642522		0	PEG	0.074	24.26	−23.31	NOT8/99	229
GB6J185328+504652		0	PEG	0.096	24.13	−22.40	NOT8/99	230
GB6J185455+735112	CJ2 1856+737	1	AGN	0.461	26.62	−25.77		231
GB6J185852+682747		–	star	–	–	–	NOT8/99	232
GB6J191212+660826		1	AGN	0.075	24.23	−23.23	INT5/99	233
GB6J192747+735755	JVASJ1927+7358	1	AGN	0.303	27.21	−25.10	NOT8/99	234
GB6J194553+705545	CJ2 1946+708	2	G	0.101	25.64	−21.90	CA7/99	235
GB6J230115+351252		0?	PEG	0.136	24.84	−22.87	INT10/99	236
GB6J235352+385549		–	star	0.000	0.00		INT10/99	237

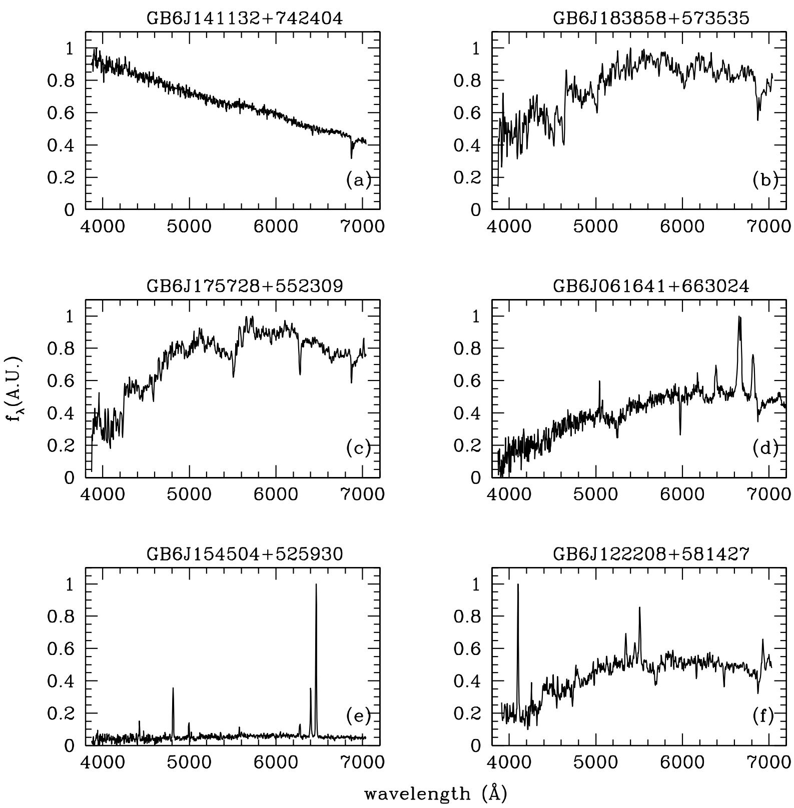

Figure 2. Examples of normalized spectra of the typical objects found in CLASS sample discussed in this paper. (a) Featureless BL Lac; (b) BL Lac candidate with a value of Δ (see section 5) between 25 and 40 per cent; (c) PEG; (d) low-redshift and low radio power type 1 AGN; (e) type 2 objects classified as AGN on the basis of the line-ratios; (f) type 2 objects classified as galaxy (probably a starburst). Fluxes are per unit of wavelength and given in arbitrary units.

reasonable fit. The additional Hα component has a width of $\sim$2000–3000 km s^{-1} and it accounts for from 30 up to 70 per cent of the total flux of the Hα + [N II] blend. The intensity ratios between the [N II]λ6583/λ6548 are found to be in the range 2–4, which is in rough agreement with the theoretical value of 3 (except for GB6J165547+444735, for which the presence of the broad Hα component does not allow one to clearly detect the [N II]λ6548 line).

In the fifth source the presence of a broad Hα component is less evident.

In conclusion, by considering the results of this analysis and by adding the objects for which a broad Hα component is claimed in the literature, for a total of 10 objects out of 21, the presence of a broad Hα component is reasonably confirmed. The remaining 11 objects are classified as 'possible type 1' ('1?' in Table 2).

4.3 Type 2

Type 2 objects include different classes of sources: Seyfert 2 galaxies, NLRGs, LINERS, H II region galaxies and starburst galaxies.

The classification of these objects is either taken from the literature, for the previously identified objects, or based on spectra obtained at the telescope, for the newly identified sources. In the latter case, the distinction between AGN (Sy2), non-AGN (H II region/starburst) and LINER was based on the diagnostic diagrams described in Veilleux & Osterbrock (1987). In any case, the quality of many of the spectra (collected mainly to find the redshift and a classification) does not allow a more accurate analysis of the observed emission lines.

In Table 2 the type 2 objects for which the presence of an AGN is suggested by the optical spectrum (Seyfert 2 galaxies, NLRG, LINERS) have been classified as 'AGN', whereas starburst or H II-region galaxies are identified with a 'G'.

4.4 The table

In Table 2, the entire list of CLASS objects which have had their spectra classified, either from the literature or during the dedicated observing runs, is presented. The following parameters are listed: (1) name (based on the GB6 position), (2) other name taken from the literature (when present), (3) type (0 = weak or no emission lines, 1 = broad emission lines, 2 = only narrow emission lines, ? = type unknown), (4) spectral classification (BL = BL Lacs, C-BL = candidate BL Lac, PEG = passive elliptical galaxy, AGN = active nucleus, G = galaxy, STAR = star (a possible mis-identification), PN = planetary nebula, SN = supernova), (5) redshift (from the literature or from specific observations), (6) total radio power at 1.4 GHz, (7) absolute R magnitude, (8) observing run, (9) reference to the notes on single objects reported at the end of the paper.

A question mark after the type number in Table 2 indicates that the spectral classification is not firm. For the 10 objects generically classified as 'galaxy' in the literature but for which an optical spectrum has not been found, the field 'type' contains just a question mark.

In Fig. 2, typical examples of spectra for some classes of objects discovered in the CLASS sample are presented. Type 0 objects (featureless BL Lacs, BL Lac candidate and PEGs) are presented in panels (a), (b) and (c), respectively. Fig. 2(d) shows the spectrum of a low radio power (and low-z) type 1 AGN with a broad Hα component in emission, and Figs 2(e) and (f) present type 2 objects classified as AGN (2e) and galaxy (probably a starburst, 2f).

In Table 3, the number of sources found in each group is reported.

Table 3. Breakdown of the optical identification.

Type	class	Number	Number $z \leqslant 0.15$
Type 0	**all**	**88**	**69(44)**[a]
	BL Lac	42	33(8)[a]
	C-BL Lac	5	2
	PEG	41	34
Type 1	**all**	**100**	**21**
Type 2	**all**	**34**	**24**
	AGN	16	9
	G	18	15
Other	**all**	**5**	
	stars[b]	3	
	PN	1	
	SN	1	
Total with classification		**227**	**114(89)**[a]
Unclassified with redshift		**10**	**10**
Unclassified		**88**	–
Total		**325**	

[a]The number of low redshift (<0.15) objects is computed assuming that the BL Lacs without a redshift estimate have $z < 0.15$. Instead, the number in parenthesis is computed assuming that the BL Lacs without a redshift have $z > 0.15$. The actual number should lie between these two values.
[b]It is likely that in these cases the object is not the true optical counterpart. The counterpart is probably fainter than the optical limit used to define the CLASS blazar survey and, thus, these three objects should not be considered anymore as part of the sample.

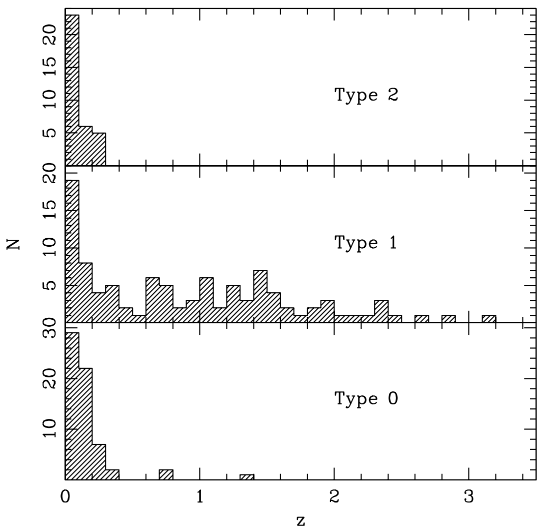

Figure 3. The redshift distribution of the three types of objects discovered in the CLASS blazar survey.

5 RADIO AND OPTICAL LUMINOSITIES

The redshift distribution of the type 0, type 1 and type 2 is reported in Fig. 3, while the radio power at 5 GHz of all the objects with an optical classification has been plotted against the absolute R

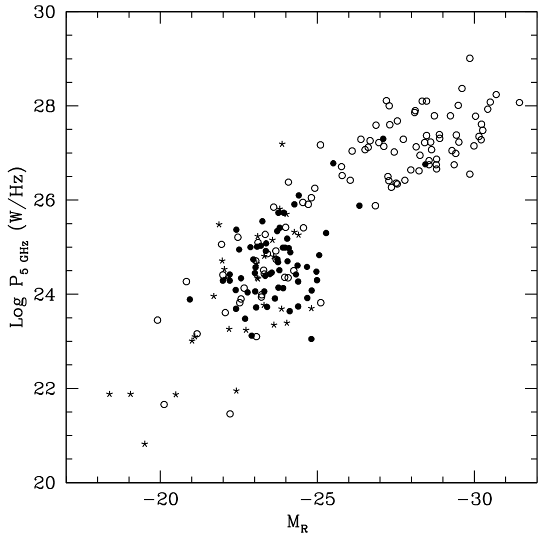

Figure 4. The radio power at 5 GHz versus the absolute *R* magnitude for the sources with a classification in the CLASS sample. Featureless BL Lacs without *z* are not included. Filled circles, open circles and stars represent type 0, type 1 and type 2 objects, respectively.

magnitude in Fig. 4. The featureless BL Lacs (without a redshift) have been excluded from this plot. Three different regimes of power can be found:

(i) a group of high radio power ($P_5 > 10^{26}\,\mathrm{W\,Hz^{-1}}$) typically composed by type 1 (open circles) and a few type 0 (filled circles) objects (BL Lac objects);
(ii) a group of low radio power ($10^{23}\,\mathrm{W\,Hz^{-1}} < P_5 < 10^{26}\,\mathrm{W\,Hz^{-1}}$). This group includes all types of objects, from type 0 to type 2; and
(iii) a few objects with a very low radio power ($P_5 < 10^{23}\,\mathrm{W\,Hz^{-1}}$). This last group contains some radio-quiet (although not radio-silent) AGNs (Seyfert galaxies) and some 'normal' galaxies whose radio emission is probably not connected to nuclear activity.

The goal of the work presented here is to select and study low-power radio-loud AGN like those found in the second group. The other two groups, i.e. the very powerful and the radio-quiet objects will not be studied in detail.

From Fig. 4 it is clear that the high power range is dominated by the type 1 objects. Nevertheless, some (33) type 1 objects are also found in the low power range ($<10^{26}\,\mathrm{W\,Hz^{-1}}$). This is surprising as it is usually assumed that low-luminosity blazars are typically featureless and devoid of a broad-line region (BLR). This result supports previous findings obtained from the analysis of the 200-mJy sample (Marchã et al. 1996) suggesting that a BLR should be present in at least a fraction of low-power blazars. In particular, two of these low-power type 1 sources discovered in the 200-mJy sample show typical blazar properties, such as a high and variable degree of optical polarization (Jackson & Marchã 1999). One of these sources (1646+499) belongs also to the CLASS blazar survey (GB6J164734+494954). The other one has a galactic latitude outside the range chosen to define the CLASS sample.

With the CLASS sample it is possible to make an estimate of the fraction of BLR in low-power objects. To this end, we have derived the luminosity functions (LF) for the total sample and for the subset composed by the type 1 objects. The two LFs are well represented by a single power law with slopes −2.11 and −2.07, respectively, for the total LF and that of type 1. The fraction of type 1 objects is then derived by integrating the two LFs between 10^{23} and $10^{26}\,\mathrm{W\,Hz^{-1}}$ and by computing the ratio between the two results.

The computed fraction is 30 per cent, when the total luminosity function is computed without the BL Lacs with no redshift. If we include also these objects assuming that they are uniformly distributed in the range of power considered here, the fraction decreases to 24 per cent. Hence, our analysis confirms the presence of a BLR in a significant fraction of low-power objects.

6 SUMMARY AND CONCLUSION

In this work the properties of a new sample of flat spectrum radio sources (the CLASS blazar survey) are presented and discussed. Three different regimes of luminosity are covered:

(i) High radio power (P_5 between 10^{26} and $10^{30}\,\mathrm{W\,Hz^{-1}}$),
(ii) Low radio power (P_5 between 10^{23} and $10^{26}\,\mathrm{W\,Hz^{-1}}$);
(iii) Very low radio power consistent with that of radio-quiet AGNs ($P_5 < 10^{23}\,\mathrm{W\,Hz^{-1}}$).

The optical classification in the different luminosity ranges is significantly different. In the high-power range the objects are typically point-like high-*z* QSOs and 'classical' BL Lacs. On the other hand, the sources that can be found in the second luminosity regime show a variety of classifications including featureless objects, optically 'normal' galaxies and broad and narrow emission line objects. Finally, the sources in the lowest luminosity group are a few NLRG and sources where starburst activity is the most important component to the optical spectrum.

The main objective of this paper is the selection and study of the low-luminosity fraction of radio-loud AGNs, i.e. those sources that fall in the second luminosity group identified here. The most interesting issue about this group of sources is that, despite the similar radio properties, such as the total power and the shape of the radio spectrum, there is much variety in spectral type ranging from BLRGs to BL Lacs and apparently 'normal' galaxies. Part of such diversity is probably due to the fact that in a sample of low-power blazars the non-thermal emission is unlikely to be the dominant component in the optical spectrum. The effect of this 'dilution' of non-thermal emission can have an important relevance in the assessment of the statistical properties of low-luminosity blazars.

An interesting result derived from the analysis of the optical properties of the objects selected in the CLASS blazar survey is that about 24–30 per cent of the low-power blazars show broad emission lines in the optical spectrum, something which is not expected because it is usually assumed that at low power the sources are devoid of a BLR. This result confirms an earlier study based on a smaller and not so deep sample of flat-spectrum radio sources (Marchã et al. 1996). The CLASS blazar sample establishes this result on a firmer statistical basis.

ACKNOWLEDGMENTS

We thank Paolo Padovani and Ian Browne for useful discussions. This research was supported by the European Commission Training and Mobility of Researchers program, research network contract ERBFMRX-CT96-0034 'CERES'. KHM, AC and MJMM are Visiting Astronomers, German-Spanish Astronomical Centre, Calar Alto, operated by the Max-Planck-Institute for Astronomy, Heidelberg, jointly with the Spanish National Commission for

Astronomy. The INT is operated on the island of La Palma by the Isaac Newton Group in the Spanish Observatorio del Roque de los Muchachos of the Instituto de Astrofisica de Canarias. The Nordic Optical Telescope is operated on the island of La Palma jointly by Denmark, Finland, Iceland, Norway, and Sweden, in the Spanish Observatorio del Roque de los Muchachos of the Instituto de Astrofisica de Canarias.

REFERENCES

Appenzeller I. et al., 1998, ApJS, 117, 319
Baan W. A., Salzer J. J., Lewinter R. D., 1998, ApJ, 509, 633
Bade N., Fink H. H., Engels D., 1994, 286, 381
Bade N., Beckmann V., Douglas N. G., Barthel P. D., Engels D., Cordis L., Nass P., Voges W., 1998, A&A, 334, 459
Beckmann V., Bade N., Wucknitz O., 1999, A&A, 352, 395
Boksenberg A., Carswell R. F., Allen D. A., Fosbury R. A. E., Penston M. V., Sargent W. L. W., 1977, MNRAS, 178, 451
Boroson T. A., Green R. F., 1992, ApJS, 80, 109
Brinkmann W., Siebert J., Reich W., Fürst E., Reich P., Voges W., Trümper J., Wielebinski R., 1995, A&AS, 109, 147
Caccianiga A., Maccacaro T., Wolter A., Della Ceca R., Gioia I. M., 1999, ApJ, 513, 51
Carilli C. L., Wrobel J. M., Ulvestad J. S., 1998, AJ, 115, 928
Carramiñana A., Guichard J., Much R., Williams O. R., 1996, A&AS, 120, 595
Condon J. J., Cotton W. D., Greisen E. W., Yin Q. F., Perley R. A., Taylor G. B., Broderick J. J., 1998, AJ, 115, 1693
Crawford C. S. C., Edge A. C., Fabian A. C., Allen S. W., Bohringer H., Ebeling H., McMahon R. G., Voges W., 1995, MNRAS, 274, 75
de Grijp M. H. K., Keel W. C., Miley G. K., Goudfrooij P., Lub J., 1992, A&AS, 96, 389
de Vaucouleurs G., de Vaucouleurs A., Corwin H. G., Jr., Buta R. J., Paturel G., Fouque P., 1991, Third Reference Catalogue of Bright Galaxies, Version 3.9 Springer-Verlag, New York
de Ruiter H. R., Parma P., Stirpe G. M., Perez-Fournon I., Gonzalez-Serrano I., Rengelink R. B., Bremer M. N., 1998, A&A, 339, 34
Downes D., Solomon P. M., Radford S. J. E., 1993, ApJ, 414L, 13
Dressler A., Shectman S., 1987, AJ, 94, 899
Engels D., Hagen H.-J., Cordis L., Koehler S., Wisotzki L., Reimers D., 1998, A&AS, 128, 507
Falco E. E., Kochanek C. S., Muñoz J. A., 1998, ApJ, 494, 47
Falco E. E. et al., 1999, PASP, 111, 438
Fleming T. A., Green R. F., Jannuzi B. T., Liebert J., Smith P. S., Fink H., 1993, AJ, 106, 1729
Gregory P. C., Scott W. K., Douglas K., Condon J. J., 1996, ApJS, 103, 427
Hagen H.-J., Engels D., Reimers D., 1999, A&AS, 134, 483
Henstock D. R., Browne I. W. A., Wilkinson P. N., McMahon R. G., 1997, MNRAS, 290, 380
Hewitt A., Burbidge G., 1993, ApJS 87, 451
Ho L. C., Filippenko A. V., Sargent W. L., 1995, ApJ, 98, 477
Ho L. C., Filippenko V., Sargent W. L. W., Peng C. Y., 1997, ApJS, 112, 391
Hook I. M., McMahon R. G., Irwin M. J., Hazard C., 1996, MNRAS, 282, 1274
Huchtmeier W. K., 1994, A&A, 286, 389
Jackson N., Browne I. W. A., 1991, MNRAS, 250, 414
Jackson N., Marchã M. J. M., 1999, MNRAS, 309, 153
Keel W. C., 1984, ApJ, 282, 75
Keel W. C., 1996, AJ, 111, 696
Kock A., Meisenheimer K., Brinkmann W., Neumann M., Siebert J., 1996, A&A, 307, 745
Kühr H., Witzel A., Pauliny-Toth I. I. K., Nauber U., 1981, A&AS, 45, 367
Landt H., Padovani P., Perlman E. S., Giommi P., Fignall H., Tzioumis A., 2001, MNRAS, 323, 757
Laurent-Muehleisen S. A., Kollgaard R. I., Ciardullo R., Feigelson E. D., Brinkman W., Siebert J., 1998, ApJS, 118, 127
Lawrence C. R., Zucker J. R., Readhead A. C. S., Unwin S. C., Pearson T. J., Xu W., 1996, ApJS, 107, 541
Machalski J., 1991, Acta Astron., 41, 1
Maoz D., Ofek E. O., Shemi A., Barth A. J., Filippenko A. V., 1996, A&A, 308, 511
Marchã M. J. M., Browne I. W. A., Impey C. D., Smith P. S., 1996, MNRAS, 281, 425
Marchã M. J. M., Caccianiga A., Browne I. W. A., Jackson N., 2001, MNRAS, 326, 1455 (Paper I)
Marziani P., Sulentic J. W., Dultzin-Hacyan D., Calvani M., Moles M., 1996, ApJS, 104, 37
Merighi R., Basso L., Vigotti M., Lahulla J. F., Lopez-Arroyo M., 1991, A&AS, 89, 225
Osmer O. S., Porter A. C., Green R. F., 1994, ApJ, 436, 6780
Padovani P., Giommi P., 1995, MNRAS, 277, 1477
Perlman E. S. et al., 1996, ApJ, 104, 251
Polomski E., Vennes S., Thorstensen J. R., Mathioudakis M., Falco E. E., 1997, ApJ, 486, 179
Rector T. A., Stocke J. T., Perlman E. S., 1999, ApJ, 516, 145
Sargent W. L. W., 1972, ApJ, 173, 7
Schmidt M., Green R. F., 1983, ApJ, 269, 352
Schneider D. P., Schmidt M., Gunn J. E., 1994, AJ, 107, 1245
Snellen I. A. G., 1997, PhD thesis, Leiden University
Snellen I. A. G., Schilizzi R. T., Bremer M. N., Miley G. K., de Bruyn A. G., Röttgering H. J. A., 1999, MNRAS, 307, 149
Stauffer J., Schild R., Keel W., 1983, ApJ, 270, 465
Stickel M., Kühr H., 1993, A&AS, 100, 395
Stickel M., Kühr H., 1994, A&AS, 103, 349
Stickel M., Kühr H., Fried J. W., 1993a, A&AS, 97, 483
Stickel M., Fried J. W., Kühr H., 1993b, A&AS, 98, 393
Stocke J. T., Morris S. L., Gioia I. M., Maccacaro T., Schild R., Wolter A., Fleming T. A., Henry J. P., 1991, ApJS, 76, 813
Ulrich M.-H., 1978, ApJ, 219, 424
Veron-Cetty M.-P., Veron P., 1996, ESO Scientific Report, 17, 1
Vermeulen R. C., Taylor G. B., 1995, AJ, 109, 1983
Veilleux S., Osterbrock E., 1987, ApJS, 63, 295
Wei J.-Y., Xu D.-W., Cao L., Zhao Y.-H., Hu J.-Y., Li Q.-B., 1998, A&A, 329, 511
White R. L. et al., 2000, ApJS, 126, 133
Wisniewski W. Z., Sitko M. L., Sitko A. K., 1986, MNRAS, 219, 299
Xu W., Lawrence C. R., Readhead A. C. S., Pearson T. J., 1994, AJ, 108, 395

APPENDIX A: NOTES ON INDIVIDUAL OBJECTS LISTED IN TABLE 2

Lines in absorption (abs.) and in emission (ems.) are listed for the objects for which we have collected a spectrum.

1 – in abs.: Ca II H and K, Mg Ib; Hα region not covered.

2 – redshift, classification and spectrum in Laurent-Muehleisen et al. (1998)

3 – in abs.: Ca II H and K, G, Hb, Mg Ib, Na ID; Hα region not covered.

4 – in abs.: Ca II H and K, G, Mg Ib; Hα region not covered.

5 – spectrum can also be found in Laurent-Mueleisen et al. (1998).

6 – no spectrum found; Brinkmann et al. (1995) classify this object as Sy1.

7 – in abs.: Ca II H and K, Hβ(?), Mg Ib, Na ID; Hα region not covered.

8 – in abs.: Ca II H and K, G, Mg Ib, Na ID; in em.: weak Hα.

9 – in abs.: Ca II H and K, G, Mg Ib, Na ID; in em.: Hβ, [O III], [O I], Hα, [N II], [S II].

10 – redshift, classification and spectrum in Henstock et al. (1997).

11 – in abs.: Mg Ib, Na ID; in em.: Hβ(?), [O III], [O I], Hα + [N II], [S II]. 12 – redshift, classification and spectrum in Osmer, Porter & Green (1994).

13 – redshift from Falco et al. (1999); classification from Ho et al. (1997); spectrum in Ho et al. (1995)

14 – star; the actual optical counterpart to the radio source must be fainter.

15 – in abs.: Ca II H and K, Mg Ib, Na I; in em.: [O II], Hα, [N II].

16 – in abs.: Ca II H and K, Mg Ib, Na ID.

17 – redshift and classification from Engels et al. (1998).

18 – redshift and classification from White et al. (2000).

19 – redshift and classification from Stickel & Kühr. (1994); spectrum in Hook et al. (1996)

20 – redshift, classification and spectrum in Laurent-Muehleisen et al. (1998).

21 – in abs.: Ca II H and K, G, Mg Ib, Na ID.

22 – spectrum in Marchã et al. (1996).

23 – redshift, classification and spectrum in Henstock et al. (1997).

24 – from QSO catalogue of Hewitt & Burbidge (1993).

25 – redshift from de Vaucouleurs et al. (1991); classified as H II galaxy in NED.

26 – spectrum in Marchã et al. (1996).

27 – redshift, classification and spectrum in Laurent-Muehleisen et al. (1998).

28 – in abs.: Ca II H and K, Mg Ib, Na ID.

29 – redshift, classification and spectrum in Wei et al. (1998).

30 – classification and spectrum in Laurent-Muehleisen et al. (1998).

31 – from QSO catalogue of Hewitt & Burbidge (1993).

32 – redshift and spectrum in Bade et al. (1998); classification and another spectrum in Perlman et al. (1996).

33 – classification from Apennzeller et al. (1998).

34 – redshift, classification and spectrum in White et al. (2000).

35 – GPS from Snellen et al. (1999); spectrum in Snellen (1997).

36 – redshift and spectrum in Lawrence et al. (1996).

37 – redshift, classification and spectrum in Stickel & Kühr (1993).

38 – from QSO catalogue of Hewitt & Burbidge (1993).

39 – in abs.: Mg Ib, Na I.; Ca II region not covered

40 – redshift and classification from Hagen, Engels & Reimers (1999).

41 – redshift and spectrum in Marchã et al. (1996).

42 – redshift and spectrum in Marchã et al. (1996).

43 – redshift from Falco et al. (1999).

44 – redshift from Falco et al. (1999).

45 – redshift and classification from Maoz et al. (1996).

46 – classification and spectrum in Henstock et al. (1997).

47 – redshift from Falco et al. (1999).

48 – classification from White et al. (2000); in em.: Hα from our spectrum.

49 – redshift and classification from Veron-Cetty & Veron (1996).

50 – redshift from de Vaucouleurs et al. (1991); LINER, Sy1.8

51 – redshift from de Vaucouleurs et al. (1991).

52 – from QSO catalogue of Hewitt & Burbidge (1993).

53 – redshift, classification and spectrum in Stickel, Fried & Kühr (1993b).

54 – redshift and classification from Veron-Cetty & Veron (1996).

55 – in em,: Mg II.

56 – redshift, classification and spectrum in Marziani et al. (1996).

57 – classification and spectrum in Laurent-Muehleisen et al. (1998).

58 – classification and spectrum in Wisniewski et al (1986) (low S/N).

59 – featureless spectrum (Fassnacht; private communication)

60 – classification and redshift from Xu et al. (1994).

61 – redshift and list of lines in Merighi et al. (1991) (only absorption features).

62 – in abs,: Ca II H and K(?), Hβ, Mg Ib, Na ID.

63 – in abs.: Ca II H and K; also in Polomski et al. (1997).

64 – redshift, classification and spectrum in Stickel & Kühr (1993).

65 – redshift and classification from White et al. (2000).

66 – featureless spectrum; also in Laurent-Muehleisen et al. (1998).

67 – in abs.: Ca II H and K, Mg Ib; in em.: [O III]; Hα region not covered.

68 – originally classified as cluster in EMSS but then re-classified as BL candidate in Rector, Stocke & Perlman (1999).

69 – redshift and classification from White et al. (2000).

70 – redshift from de Vaucouleurs et al. (1991).

71 – redshift, classification and spectrum in Bade et al. (1998); Marchã et al. (1996) give a different (probably not correct) redshift.

72 – redshift, classification and spectrum in Jackson & Browne (1991).

73 – redshift, classification and spectrum in Hook et al. (1996).

74 – spectrum in Marchã et al. (1996).

75 – in abs.: Mg Ib, Na I; in em.: weak [O III], [N II], Hα; Ca II region not covered.

76 – redshift and classification from NED research team.

77 – redshift, classification and spectrum in Laurent-Muehleisen et al. (1998); redshift uncertain

78 – in abs.: Ca II K and H, G, Hβ, Mg Ib; Hα region not covered.

79 – redshift from Falco et al. (1999); spectrum in Ho et al. (1995)

80 – spectrum of host galaxy in Ulrich (1978); featureless spectrum (Sargent 1972).

81 – redshift from Bade, Fink & Engels (1994); spectrum in Laurent-Muehleisen et al. (1998).

82 – z (NED) based on low-dispersion spectroscopy (Schneider, Schmidt & Gunn 1994); possibly type 1.

83 – redshift from de Vaucouleurs et al. (1991).

84 – in abs.: Ca II H and K, G, Mg Ib, Na ID; Hα region not covered.

85 – redshift and spectrum in Marchã et al. (1996).

86 – redshift and spectrum in Marchã et al (1996).

87 – redshift and spectrum in Henstock et al. (1997).

88 – in em.: C IV, C III].

89 – featureless; also in Laurent-Muehleisen et al. (1998).

90 – redshift from Falco et al. (1999); spectrum in Ho et al. (1995); broad Hα(?); classification in NED is Sy1-LINER.

91 – no spectrum available; classified as BL Lac in Padovani & Giommi (1995).

92 – redshift from Falco, Kochanek & Muñoz (1998); classified as LINER in NED (no spectrum available).

93 – redshift, classification and spectrum in Laurent-Muehleisen et al. (1998).

94 – classification and spectrum in Henstock et al. (1997).
95 – redshift from de Vaucouleurs et al. (1991).
96 – SN in NGC4157 (NED).
97 – redshift from de Vaucouleurs et al. (1991).
98 – redshift from Falco et al. (1999); spectrum in Ho et al. (1995).
99 – in em.: Mg II; ($z = 2.225$ in NED).
100 – in abs.: Mg Ib; in em.: [O II], [He III], Hγ, Hβ, [O III], [O I]; Hα region not covered
101 – redshift from Falco et al. (1999).
102 – in em.: Mg II, C III](?).
103 – redshift and list of lines in Merighi et al. (1991).
104 – redshift from QSO catalogue of Hewitt & Burbidge (1993).
105 – redshift from Falco et al. (1998); only absorption lines from Falco et al. (1998).
106 – redshift, classification and spectrum in Machalski (1991).
107 – in abs.: Ca II H and K, G, Mg Ib; in em.: [O III]; Hα region not covered.
108 – redshift and classification from Falco et al. (1998).
109 – redshift and spectrum in Marchã et al. (1996).
110 – no spectrum available; classification from Appenzeller et al. (1998).
111 – redshift and spectrum in Marchã et al. (1996).
112 – featureless; also classified as BL Lac in Fleming et al. (1993)
113 – featureless (tentative $z = 0.05$); also classified as BL Lac in Henstock et al. (1997).
114 – redshift from Carilli, Wrobel & Ulvestad. (1998); spectrum in Boksenberg et al. (1977).
115 – in abs.: Ca II H and K; in em.: [O II], [O III], Hα + [N II], [S II].
116 – in abs.: Na I,Mg Ib; in em.: [O III], [N II], Hα; Ca II region not covered.
117 – featureless.
118 – redshift and spectrum in Merighi et al. (1991).
119 – redshift, classification and spectrum in Boroson & Green (1992)
120 – redshift from Falco et al. (1999); spectrum in Ho et al. (1995); classification (Sy1.5) from Ho et al. (1997).
121 – in em.: C IV, C III].
122 – in abs.: Ca II H and K, G, Mg Ib, Na ID; in em.: very weak Hα, [S II].
123 – redshift from QSO catalogue of Hewitt & Burbidge (1993).
124 – in abs.: Ca II H and K, G, Mg Ib
125 – in abs.: Ca II H and K, G, Mg Ib, Na ID.
126 – redshift from Downes, Solomon & Radford (1993); classified as Sy2 in NED; Spectrum in Baan, Salzer & Lewinter (1998)
127 – redshift from de Vaucouleurs et al. (1991).
128 – redshift from Falco et al. (1999); classification (Liner or Sy2) in Ho et al. (1997); spectrum in Ho et al. (1995).
129 – redshift and list of lines in Xu et al. (1994).
130 – in em.: [O II], [Ne III], Hb, [O III].
131 – in abs.: Ca II H and K, Mg Ib, Na ID; in em.: very weak Hα.
132 – redshift from Huchtmeier 1994; spectrum in Ho et al. (1995): Ca II region not covered.
133 – redshift, classification and spectrum in Laurent-Muehleisen et al. (1998).
134 – in em.: Mg II?, O III?, [NeV]? (tentative redshift).
135 – featureless; very tentative $z = 0.46$.
136 – redshift, classification and spectrum in Laurent-Muehleisen et al. (1998).
137 – redshift and spectrum in Crawford et al. (1995).
138 – redshift, classification and spectrum in Laurent-Muehleisen et al. (1998).
139 – redshift, classification and spectrum in Stickel et al. (1993b).
140 – redshift and spectrum in Marchã et al. (1996).
141 – in abs.: Ca II H and K, G, Mg Ib, Na ID;in em.: weak [O III]
142 – in em.: Mg II.
143 – redshift from Falco et al. (1999); spectrum in Keel (1984).
144 – redshift and classification from QSO catalogue of Hewitt & Burbidge (1993).
145 – redshift computed assuming the observed emission line is Mg II.
146 – redshift, classification and spectrum in de Grijp et al. (1992).
147 – redshift, classification and spectrum in Laurent-Muehleisen et al. (1998). Confirmed by our observations
148 – in abs.: Ca II H and K, G, Mg Ib, Na I.
149 – redshift and classification from de Ruiter et al. (1998).
150 – redshift from Falco et al. (1999); spectrum in Ho et al. (1995).
151 – featureless; redshift from Beckmann, Bade & Wucknitz (1999).
152 – LINER+H II; triple system: CLASS position (8.4 GHz) is on northern object.
153 – in abs.: Mg Ib, Na I; in em.: [N II], Hα, [S II].
154 – redshift and spectrum in Laurent-Muehleisen et al. (1998); Hα classified as broad.
155 – in em.: SiIV/O IV], C IV, C III].
156 – 2 objects; CLASS position (8.4 GHz) on QSO; redshift from Vermeulen & Taylor (1995) (QSO); spectrum in Stickel, Kühr & Fried (1993a).
157 – in abs.: Ca II H and K, Gb, Mg Ib, Na ID; in em.: broad Hα. From Vermeulen, Browne & Fassnacht (private communication).
158 – featureless; also in Laurent-Muehleisen et al. (1998)
159 – in abs.: Mg Ib, Na I; in em.: [O III], Hα, [N II], [S II]; Ca II region not covered.
160 – in em.: [Ne V], [O II], [Ne III], Hβ, [O III].
161 – redshift, classification and spectrum in Snellen et al. (1999).
162 – in abs.: Ca II H and K, Hβ, Mg Ib, Na ID, Hα.
163 – only abs. lines (from Falco et al. 1998)
164 – redshift and spectrum in Marchã et al. (1996).
165 – in abs.: Ca II H and K, G, Hβ, Mg Ib; Hα region not covered.
166 – in em.: C III], Mg II
167 – redshift from QSO catalogue of Hewitt & Burbidge (1993).
168 – in em.: Hγ, Hβ, [O III], Hα.
169 – in em.: C III], Mg II.
170 – redshift from Veron-Cetty & Veron (1996); redshift confirmed by our observations.
171 – in abs.: Ca II H and K, G, Hβ, Mg Ib, Na ID
172 – in em.: C III], Mg II; also in Appenzeller et al. 1998
173 – redshift and spectrum in Snellen et al. (1999).
174 – redshift and classification in Brinkmann et al. (1995).
175 – in abs.: Ca II H and K, G, Mg Ib, Na Id; in em.: weak Hα.

176 – redshift, classification and spectrum in Laurent-Muehleisen et al. (1998).

177 – redshift, classification and spectrum in Landt et al. (2001).

178 – redshift from Falco et al. (1999); no spectrum available.

179 – redshift, classification and spectrum in Marziani et al. (1996).

180 – spectrum in Snellen (1997); redshift confirmed by the our observations

181 – redshift, classification and spectrum in Marziani et al. (1996).

182 – redshift, classification and spectrum in Kock et al. (1996).

183 – redshift and spectrum in Marchã et al. (1996).

184 – redshift, classification and spectrum in White et al. (2000).

185 – redshift and spectrum in Marchã et al. (1996).

186 – in abs.: Ca II H and K, G, Mg I b; in em.: [O II], [O I], Hα, [S II].

187 – redshift and classification from Hewitt & Burbidge (1993); no spectrum available.

188 – in abs.: Ca II H and K, G, Mg I b; in em.: [O II], Hβ, [O III]; Hα region not covered

189 – featureless.

190 – featureless (but spectrum very noisy).

191 – redshift and classification from QSO catalogue of Hewitt & Burbidge (1993).

192 – in abs.: Mg I b, Na I; in em.:Narrow & weak Hα + [N II].

193 – redshift from QSO catalogue of Hewitt & Burbidge (1993).

194 – in abs.: Mg I b, in em. [O II], Hβ, [O III], Hα + [N II], [S II]; magnitude is uncertain due to blending;

195 – in abs.: Ca II H and K, G, Mg I b; in em.: [O III], Hα + [N II].

196 – redshift from Keel (1996); spectrum in Stauffer, Schild & Keel (1983).

197 – redshift and classification in Schmidt & Green (1983).

198 – in abs.: Ca II H and K, G, Mg I b, Na I D; Hα region not covered.

199 – redshift, classification and spectrum in White et al. (2000).

200 – in em.: C III], Mg II.

201 – featureless.

202 – in em.: [O II], Hγ, Hβ, [O III].

203 – redshift from in de Vaucouleurs et al. (1991).

204 – redshift and classification from QSO catalogue of Hewitt & Burbidge (1993).

205 – poor S/N; possible BL Lac.

206 – in abs.: Ca II H and K, Mg I b.

207 – in abs.: Ca II H and K, Mg I b, Na I D.

208 – in abs.: Ca II H and K, Mg I b; in em.: very weak Hα or [N II].

209 – also in Laurent-Muehleisen et al. (1998).

210 – redshift from Falco et al. (1999); spectrum Carramiñana et al. (1996).

211 – redshift, classification and spectrum in Stickel et al. (1993b).

212 – classification and spectrum in Henstock et al. (1997)

213 – redshift, classification and spectrum in Laurent-Muehleisen et al. (1998).

214 – redshift and spectrum in Marchã et al. (1996).

215 – in abs.: Ca II H and K, Mg I b; in em.: [O II].

216 – redshift and spectrum in Laurent-Muehleisen et al. (1998); Hα region not covered.

217 – in abs.: Ca II H and K, G, Mg I b, Na I D; in em.; very weak [O II], [N II].

218 – from NED.

219 – classification and redshift from QSO catalogue of Hewitt & Burbidge (1993).

220 – in abs.: Ca II H and K, Mg I b; in em.: Hα + [N II].

221 – in abs.: Ca II K, Mg I b, Na I D; in em.: possibly a weak Hα(?).

222 – redshift and spectrum in Marchã et al. (1996).

223 – in em.: C III], Mg II.

224 – in em.: C III], Mg II.

225 – redshift, classification and spectrum in Laurent-Muehleisen et al. (1998).

226 – in abs.: Ca II H and K, G, Mg I b

227 – tentative z.

228 – redshift, classification and spectrum in Stickel & Kühr (1993).

229 – in abs.: Ca II H and K, Mg I b, Na I D.

230 – in abs.: Ca II H and K, Mg I b, Na I D.

231 – redshift and spectrum in Henstock et al. (1997).

232 – optical object 4″ away from the NVSS position ; not detected at 8.4 GHz.

233 – in abs.: Ca II H and K, G, Mg I b, Na I D; in em.: [O II], [O III], [O I], Hα+[N II], [S II].

234 – in em.: [NeIII], He, Hδ, Hγ, Hβ, [O III], Hα; classified in NED as QSO/BLLAC/LPQ

235 – spectrum in Henstock et al. (1997) and z confirmed by CA observations. Narrow Hα in emission

236 – in abs.: Ca II H and K, G, Mg I b; in em.: Hβ?, [O III]?; Hα region not covered.

237 – star; the real optical counterpart to the radio source must be fainter.

This paper has been typeset from a TEX/LATEX file prepared by the author.